

# NPP Estimation Using Unmanned Helicopter and Satellite Observation Data on Cedar Forest in Japan

Shinobu Furumi<sup>1</sup>, Lu Chen<sup>1</sup>, Kanako Muramatsu<sup>2</sup>, Yan Xiong<sup>1</sup>, Yoshiaki Honda<sup>3</sup>, Noboru Fujiwara<sup>1</sup>

<sup>1</sup> Department of Information and Computer Sciences, Nara Women's University, Nara, Japan

<sup>2</sup> KYOUSEI Science Center, Nara Women's University, Nara, Japan

<sup>3</sup> Center for Environmental Remote Sensing(CEReS), Chiba University, Chiba, Japan

Tel: +81-742-20-3738, FAX: +81-742-20-3739, e-mail: awa@ics.nara-wu.ac.jp

## ABSTRACT

The purpose of this study is to examine the Net Primary Production (NPP) using the data of the satellite. So we carried out the measurement of reflectance(the wavelength is from 520nm to 920nm) by helicopter on an cedar forest in Nara, Japan in July, 2002. Sensor onboard the helicopter observed the BRF of an area of cedar forest and the reflectance of several different area at nadir of sensor. We examined the relationship between reflectance and opening angle of sensor observation and solar illumination angle. When the opening angle is zero, the reflectance is the highest due to less shadow. Taking into account the relationship, by the developed PDM (Pattern Decomposition Method), we can calculate the VIPD from the reflectance. And then we can estimate the NPP from the VIPD value. average NPP per a month of July, 2002 of the cedar forest was estimated to be  $0.338kg \cdot CO_2/m^2$ .

**KEYWORDS:** BRF, Photosynthesis, Cedar forest, Helicopter, Vegetation index

## 1 BACKGROUND

The Advance Earth Observing Satellite-II(ADEOSII) was launched at 10:31 a.m. on Dec,14 in 2002 (Japan Standard Time) from the Tanegashima Space Center by the National Space Development Agency of Japan(NASDA). For estimating the NPP(Net Primary Production) using the data of the global imager(GLI) which is loaded with ADEOSII, we developed a NPP estimation method using a vegetation index based on pattern decomposition. For validation and modification of the estimation method, we carried out the measurement of the spectral reflectance by unmanned helicopter on cedar forest in Nara, Japan in July, 2002. And at the same time, we do the spot exploration every month since July, 2002. We expect to estimate the growth of the trees per year by the spot exploration. And ultimately, we would like to obtain the result by comparing the NPP estimation from the spot exploration, with the NPP estimation from the helicopter observation and with the NPP estimation from the data of the satellite Landsat.

## 2 HELICOPTER OBSERVATION

### 2.1 About the Helicopter Observation

The wavelength range of the helicopter observation is from 520nm to 920nm. The field of view is  $20^\circ$  and the flight altitude is about 40m, so the instantaneous field of view is  $14\text{m} \times 14\text{m}$ . The observation area is a cedar forest which is located in Nara Prefecture of Japan. Cedar is major tree in this forest. The age of the trees is about 36 years. The stand density is 1732 trees/ha and the average height of the trees is 12.77m. This forest is on the  $35^\circ$  slope facing southwest.

The helicopter observation lasted three days which was from July,16 to July,18. We used two ways to measure the spectral reflectance by helicopter. One is called mosaic observation, and the other is called BRF observation.

Mosaic is a method that the helicopter is always vertically above the objective in the course of observing. And the objective is continuous, just as shown in Fig. 1. There are 24 observation points in this mosaic observation. We carried out the mosaic observation one time per day on July,16 and July,17. We describe 24 observation points of mosaic observation on July,16 as depicted in Fig. 2.

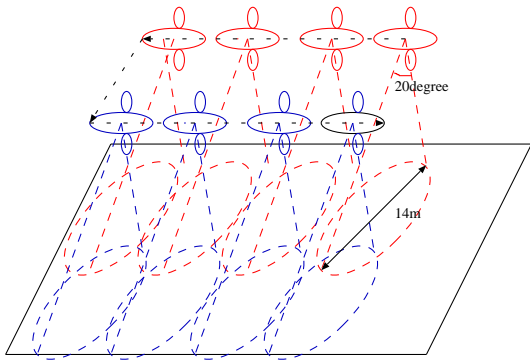


Figure 1: the imagination of mosaic observation

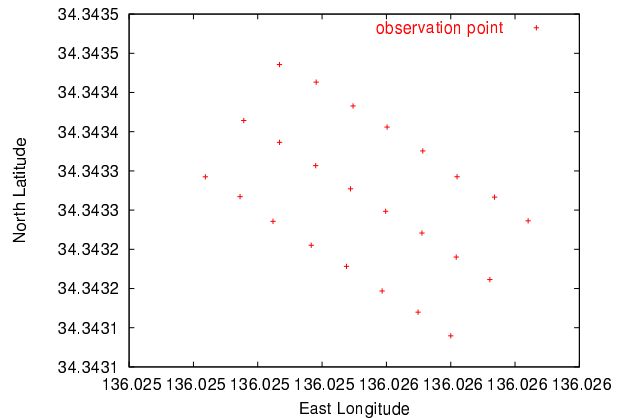


Figure 2: Illustration of 24 observation points of mosaic observation on July,16.

BRF(Bidirectional Reflectance Factor) observation is to measure the spectral reflectance as to the same objective by the different directions. BRF depends on the direction of the source of light and the direction of the sensor. We simply illustrate BRF observation in Fig. 3. We carried out the BRF observation three times on July,18. For example, 33 observation points of the first time observation on July,18 is represented in Fig. 4. The center objective of this BRF observation is about the field at point 9. The sensor loaded in the helicopter is in the principle plane with solar for observation point 1 ~ 17 and the sensor is in the vertical plane with solar for observation point 18 ~ 33.

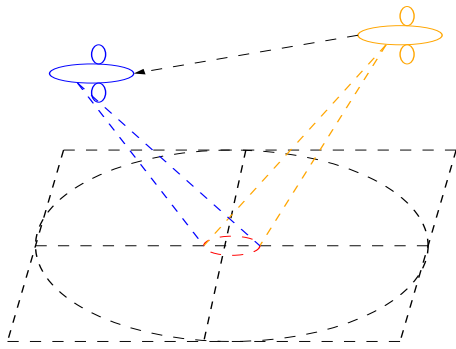


Figure 3: the imagination of BRF observation

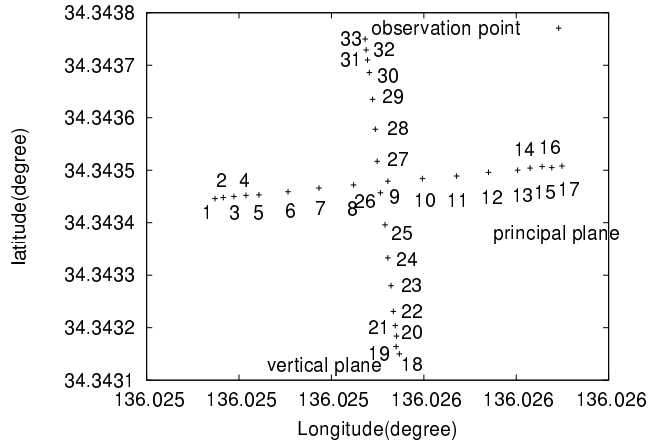


Figure 4: Illustration of 33 observation points of the first observation on July,18.

## 2.2 Feature of reflectance data on cedar forest

We measured the spectral reflectance of the cedar leaves by FieldSpec on July,18 2002. The reflectance of the cedar leaves is shown in Fig. 5 by the broken line and the other line is the reflectance measured by helicopter at observation point1 in the first observation on July,18. we can find that the reflectance by helicopter is much lower than the the reflectance by FieldSpec. We assume that the difference of the reflectance is relationship with the difference of the distribution of the objective leaves by FieldSpec and by helicopter.

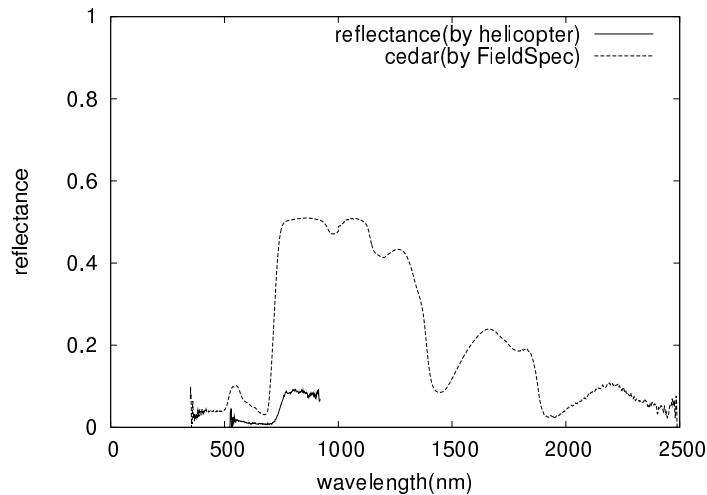


Figure 5: The long-dotted line indicates the reflectance of the cedar leaves by FieldSpec. The other line indicates the reflectance by helicopter.

In Fig. 6, the left photo was the target area that taken by the digital camera on

the helicopter at point1 of BRF observation of target area. The right photo was taken at point 12. In the figure below, the broken line is the reflectance corresponding to the left photo. And the dotted line is the the reflectance corresponding to the right photo. Comparing the two pieces of photo and the figure, we would find that the values of the reflectance are quite different even if they are both measured by the helicopter.

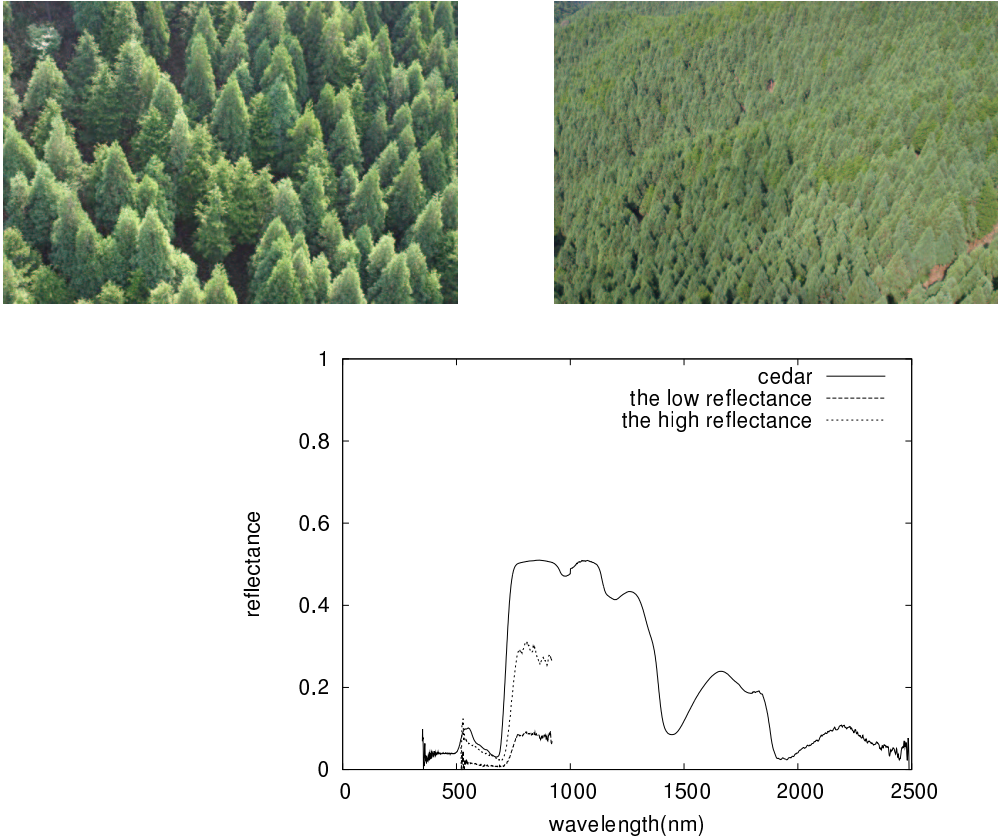


Figure 6: The left photo is taken at point 1 of the first observation on July. 18 and the right photo is taken at point 12. The broken line is the reflectance at point 1 and the dotted line is the reflectance at point 12. The other line is the reflectance of cedar by FielSpec.

If we look over the two pieces of photo more deeply, we would find that there is a lot of shadow in the left photo which is corresponding to the low reflectance. So we could think one more reason that making the spectral reflectance by helicopter low is the shadow.

### 2.3 Considering the effect by shadow

Here, we define the opening angle as the angle between the observation direction of sensor and illumination direction from solar. We try to find the relationship between the reflectance and the opening angle. And assume that when the opening angle is equal to  $0^\circ$ , the reflectance is without the effect by shadow.

We would take the first observation on July,18 as the example to explain how to find the relationship between the reflectance and the opening angle. From Fig. 4, we could consider the sensor is in the principle plane with the solar at from point 1 to point 17 and the sensor is in the vertical plane with the solar at from point 18 to point 33. We choose point 1 ~ 17 to study the relationship. As mentioned before, the center objective of the observation is almost in the field at point 9. We divide 17 points into two groups to study . One group including point 9 ~ 17 is that the sensor is in the same plane with solar, so the opening angle is equal to solar zenith angle ! <the zenith angle of sensor. And the other group including point 1 ~ 8 is not in the same plane with solar, so the opening angle is equal to solar zenith angle ! \the zenith angle of sensor. As depicted in Fig. 7, the opening angle could be easy to be calculated.

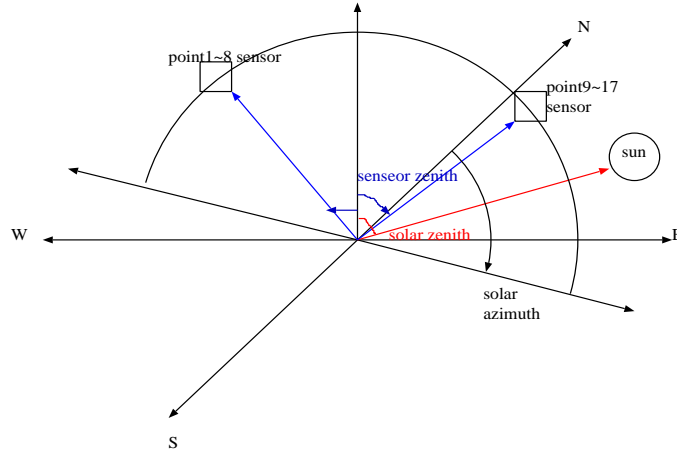


Figure 7: The definition of the opening angle! the opening angle  $\theta = \text{Solar zenith} \pm \text{Sensor zenith}$

We can calculate the opening angle at every point. By the same way, we could know the relationship between the reflectance and the opening angle of the second and the third time observation on July,18. And then we obtain Fig. 8 which is including the relationship between the reflectance at about 800nm as example and the opening angle of the three times observation on July,18. Just as the assumption, when the opening angle is  $0^\circ$ , the reflectance is the highest.

### 3 ESTIMATING THE VALUE OF VIPD AND NPP

The object of this paper is to estimate the value of NPP of the selected cedar forest. But for the value of NPP, we must calculate the value of VIPD (Vegetation Index based on Pattern Decomposition). We would like to estimate the value of VIPD of BRF observation with the reflectance of the first time observation on July,18. As to the mosaic observation, we would try to estimate VIPD by using the reflectance measured in three times in BRF.

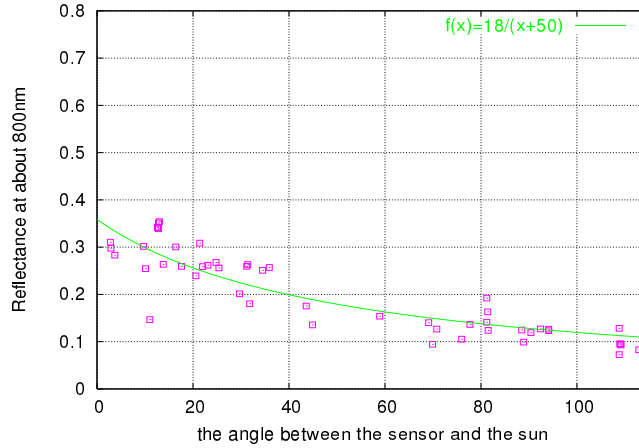


Figure 8: Illustration of the relationship between the reflectance and the opening angle of the three times observation on July,18. We take the opening angle as  $x$  and the reflectance as  $y$ , and then fit the equation  $y=b/(x+a)$ . The result  $y=18/(x+50)$  is expressed by curve

### 3.1 The selection of the GLI bands

GLI has 36 bands. Corresponding to the wavelength range(520nm~ 920nm) of the helicopter observation and the objective of every band, we choose five bands to calculate VIPD. And the five bands are band 8(center wavelength 545nm), band 13(center wavelength 678nm), band 15(center wavelength 710nm), band 17(center wavelength 763nm), band 19(center wavelength 865nm).

### 3.2 About PDM(Pattern Decomposition Method)

We have developed a new analysis method for multi-spectral satellite data called "Pattern Decomposition Method"(PDM). The PDM is one type of spectral mixing analysis but the spectrum of each pixel is basically expressed as the linear sum of fixed three standard spectral patterns, namely the spectral patterns of three representative land objects: water, vegetation, and soil. In the PDM, these three patterns have no meaning of special classification category but are standard spectral pattern components of general spectra. The spectral pattern for most ground objects can be reconstructed by the three standard patterns. The following figure shows the continuous spectrum of the selected three standard patterns and the selected GLI 5 bands.

Then we calculate the mean reflectance of the three standard patterns which is corresponding to the selected GLI bands. In order to know the standardized reflectance, we suppose the values of reflectance of 5 selected GLI bands of every standard pattern as 1, and then to calculate the coefficient that is the rate of the every value of reflectance of 5 selected GLI bands of every standard pattern. The result is shown in Fig. 10.

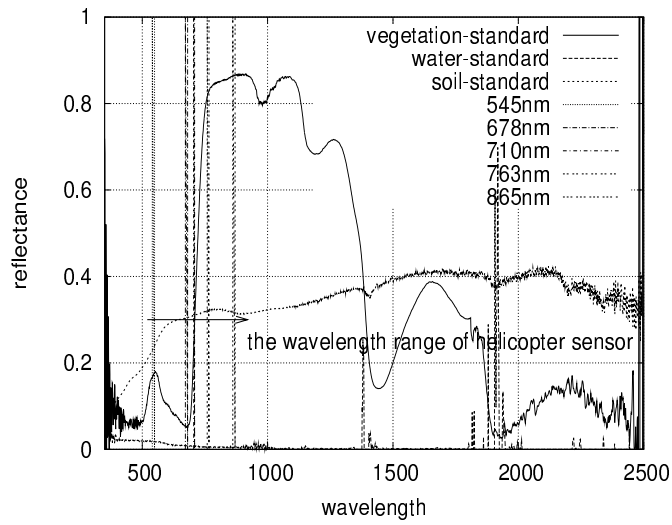


Figure 9: The lengthwise lines indicates the continuous spectrum of the three standard patterns and the crosswise lines indicates the selected GLI bands. The arrow means the wavelength range of helicopter sensor.

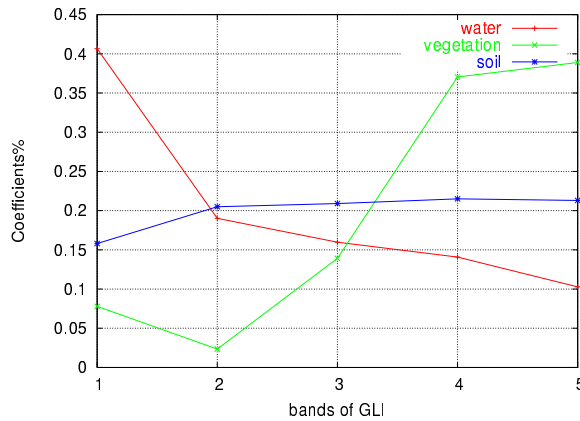


Figure 10: Illustration of the standardized reflectance of the three standard patterns corresponding the 5 GLI bands

### 3.3 VIPD by BRF observation data

We would like to take the first observation on July, 18 as an example to calculate the value of VIPD of BRF observation. As to the center objective in that observation, we can calculate the corresponding coefficient ( $C_w, C_v, C_s$ ) of the pattern decomposition and then VIPD (Vegetation Index based on Pattern Decomposition) can be estimated. That is to say, VIPD of that observation is VIPD of the field at point 9. Fig. 11 is represented that VIPD of center objective estimated from the reflectance which is measured at points 1 ~ 17.

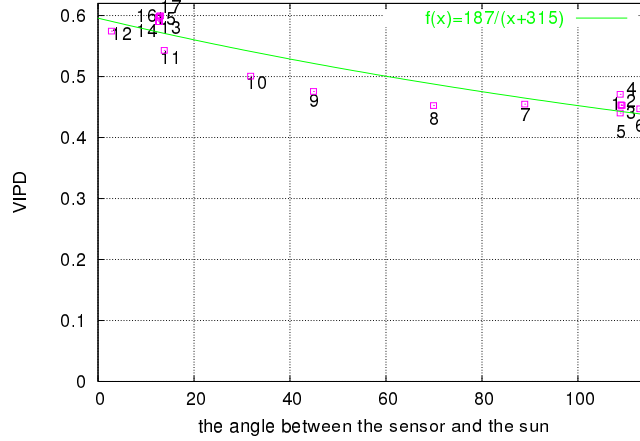


Figure 11: Illustration of the relationship between VIPD and the opening angle. The x-axis is the opening angle and the y-axis is the value of VIPD at every point. We take the opening angle as  $x$  and VIPD as  $y$ , and then fit the equation  $y = b / (x + a)$ . The result  $y = 28 / (x + 30)$  is expressed by curve.

### 3.4 Obtaining the reflectance without the effect by shadow in mosaic observation

Just as mentioned before, we try to remove the effect of shadow by the opening angle in the mosaic observation. We could believe there is no effect of the shadow when the opening angle is  $0^\circ$ . expect that we can know the different coefficient at different wavelength range. From Fig. 8, we can know the reflectance of BRF is equal to 0.36 when the opening angle is  $0^\circ$ . And since most of the opening angle in mosaic observation are from 67 to 69, we can get the reflectance is 0.153 when the opening angle is 68 (the mean opening angle in mosaic observation). So we might think that the reflectance of mosaic observation should be magnified 2.35 ( $0.36 / 0.153$ ) times in order to remove the effect by shadow. The magnified reflectance at every point of mosaic observation is illustrated in Fig. 12.

Since the field of every observation point of mosaic observation is different, we need to calculate VIPD at every point. The value of VIPD which is estimated from the magnified reflectance before in mosaic observation are shown in Fig. 13.



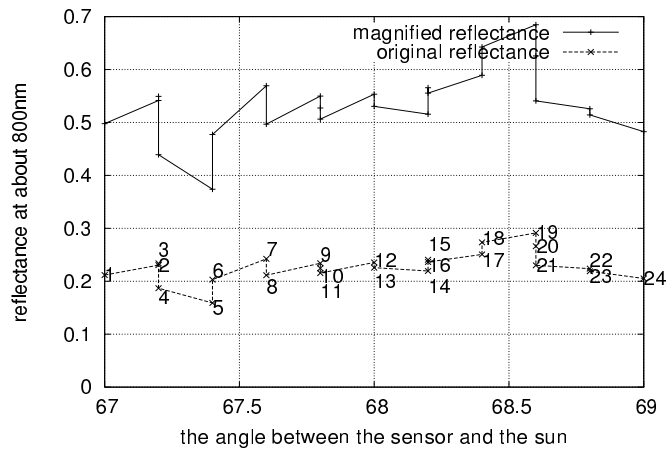


Figure 12: Illustration of the magnified reflectance. The broken curve is the original reflectance and the other curve is the magnified curve.

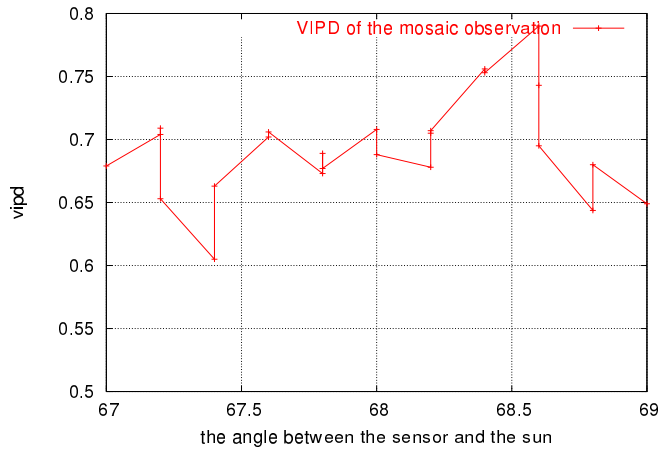


Figure 13: Illustration of VIPD of the mosaic observation.

### 3.5 NPP estimation

Based on the relationship between reflectance and opening angle, we can obtain a vegetation index VIPD without shadow effects. In this section, average NPP per a month of July, 2002 is estimated from VIPD from BRF observation and mosaic observation.

#### 3.5.1 Estimation method of NPP

We would like to introduce the method of estimating the NPP. The calculating expression of NPP is shown as following:

$$NPP = GPP - Rd \quad (1)$$

$$GPP(\text{GrossPrimaryProduction}) = \int \frac{VIPD(t)}{VIPD_{std}} P_{std}(PAR)(t) dt \quad (2)$$

$$P_{std}(PAR)(t) = \frac{0.53 \times 0.027 \times PAR(t)}{1 + 0.027 \times PAR(t)} \quad (3)$$

$$VIPD_{std} = 0.561 \quad (4)$$

$$Rd = \frac{7.825 + 1.145T(t)[^{\circ}C]}{100} \times (GPP) \quad (5)$$

In expression(2), VIPD<sub>std</sub> means the standard value of VIPD. In expression(2), PAR is Photosynthetic Active solar Radiation and which is equal to 0.39× the global solar irradiance. The coefficient 0.39 is estimated from the mean value of the data measured in Mongolia and Wuhan and the building in Nara Womens University. In expression(4), Rd indicates the loss of production because of the respiration. T is the mean temperature. VIPD<sub>std</sub> and P<sub>std</sub>(PAR) are determined by the ground measurement for several leaves.

#### 3.5.2 NPP estimation by BRF measurement data

From Fig. 11, we can understand that when the opening angle is equal to 0°(as mentioned before, we can consider there is no the effect by shadow at that time), the value of VIPD is about 0.59. So in expression(2), VIPD is equal to 0.59.

We use the data of the global solar irradiance which was obtained in July,2002 on the roof of a building in Nara Womens' University.

From the method mentioned before, we integrate the value of NPP in each time. For obtaining the value of GPP in each time, we must calculate the mean PAR in each time by using the mean the global solar irradiance in each time. Then the amount of breathing in each time can be calculated by putting the value of GPP and the temperature of each time into the expression. Finally, we can obtain the value of NPP is 0.35kg·CO<sub>2</sub>/m<sup>2</sup>·month by integrating the value of NPP in each time.

On the other hand, we always have not enough data just as the mean global solar irradiance per day and others. We can use the daylight hours and the mean daily global solar irradiance and the aera mean temperature to estimate NPP. Considering the daylight hours is 12 hours, the mean value of the global solar irradiance is  $402W/m^2$ . Here, we think the mean temperture in July in Nara is  $25.0^\circ$ , and applying to the expression(1)~(5), we can know the value of NPP is  $0.384kg\cdot CO_2/m^2\cdot month$ .

We could find it is very close between the NPP by considering 12 hours as the daylight hours and the integral NPP.

### 3.5.3 NPP estimation by mosaic observation

By using the mean temperature  $25.2^\circ$ , and using the daylight hours such as 12 hours, NPP can be achieved as shown in Fig. 14. The average value of NPP by mosaic observation is  $0.338kg\cdot CO_2/m^2\cdot month$ .

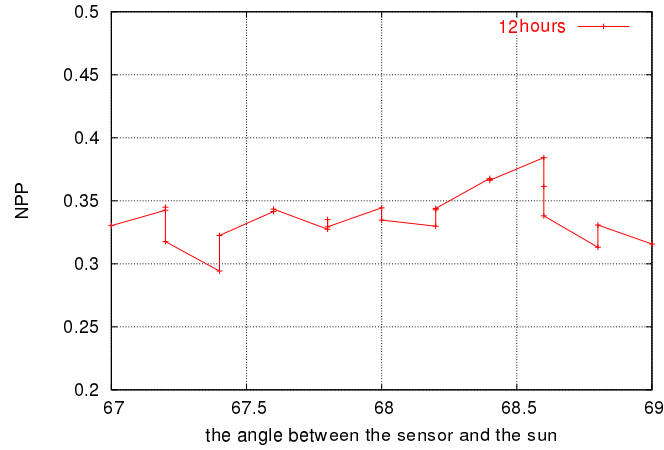


Figure 14: Illustration of NPP of the mosaic observation

## 4 CONCLUSION

By the two methods of the helicopter observation, we found the features of BRF observation. At the same time, we could obtain the reflectance without the effect by shadow of mosaic observation by using the features of BRF observation. And then we could estimate the value of NPP with the reflectance without the effect by shadow. The average NPP per a month of July, 2002 of ceder forest in Japan was estimated to be  $0.338kg\cdot CO_2/m^2$ .

Now we continue the spot exploration every month which is including measuring diameter at breast height, the tree height and so on. Although one year has passed, we have not enough data to estimate NPP. We expect to estimate NPP by this way.

We would also like to estimate NPP by using the data of satellite Landsat/ETM×. And finally, we can compare the three values of NPP by the helicopter observation and the spot exploration and satellite.

## ACKNOWLEDGEMENTS

This work was supported under the ADEOS-II/GLI project by the National Space Development Agency of Japan(NASDA).

## REFERENCE

- N. Fujiwara, K. Muramatsu, S. Awa, T. Hazumi, and F. Ochiai (1996). "Pattern expand method for satellite data analysis (in Japanese)", *Journal of The Remote Sensing Society of Japan*, 16(4)41-49, 1996
- S. Furumi, A. Hayashi, K. Muramatsu, and N. Fujiwara (1998). "Relation between vegetation vigor and a new vegetation index based on pattern decomposition method", *Journal of The Remote Sensing Society of Japan*, 18(3)17-34
- S. Furumi, Y. Xiong, and N. Fujiwara (Submitted), Establishment of an algorithm to estimate canopy photosynthesis by pattern decomposition using multi-spectral data, *Journal of The Remote Sensing Society of Japan*
- A. Hayashi, K. Muramatsu, S. Furumi, Y. Shiono, and N. Fujiwara (1998). "An algorithm and a new vegetation index for ADEOS-II/GLI data analysis", *Journal of The Remote Sensing Society of Japan*, 18(2)28-50
- K. Muramatsu, S. Furumi, A. Hayashi, N. Fujiwara, M. Daigo, and F. Ochiai(2000). "Pattern decomposition method in the albedo space for Landsat/TM and MSS data analysis", *International Journal of Remote Sensing*, 21(1)99-119